

# Extending uptimes for tugs with the Voith Schneider Propeller (VSP) Case study





# Extending uptime for tugs

**SEAKEEPING BEHAVIOUR** Rolling movements are often the limiting factor for tug operations in waves. However, the Voith Schneider Propeller (VSP) with its fast and dynamic thrust adjustment, enables efficient active roll stabilisation and dynamic positioning (DP). This opens up new opportunities to increase the efficiency of tug operations, write Dr Dirk Jürgens and Michael Palm from Germany's Voith GmbH.



Figure 1: Voith Water Tractor, *Forte*, equipped with two Voith Schneider Propellers (VSP36EC) and the electronic Voith Roll Stabilization (VRS)

Source for all images and figures: Voith

Tug rolling motions are often the limiting factor in offshore applications. While the waves counter LNG carriers from an optimal direction – from bow or stern – tugs often have to operate under the worst beam wave conditions. At a moderate significant wave height of  $H_s = 1.9\text{m}$ , roll angles of up to  $26.7^\circ$  were measured [5], with significant implications for crew welfare and productivity.

The VWT or RAVE Tug is a well-proven design and the Carrousel Rave Tug (CRT) [6] offers scope to deploy active Voith Roll Stabilization (VRS). As a result, roll movements can be reduced considerably, by as much as 70% on tugs. The basis for the VRS is the fast response of the VSP [7], [8].

This article explains the effect of VRS using calculations, model tests and customer feedback as examples. The conclusion is that through the targeted use of VRS to reduce roll, the operating times of offshore tugs can be significantly ex-

Tugs must now work in bigger waves because today's larger vessels require them to make line connections earlier, particularly in areas where considerable waves build up [1]. But the effect of waves can be detrimental to the seakeeping characteristics of tugs, including limitations due to rolling motions, fluctuating line forces and the reduction of propeller forces due to ventilation and inflow speed to the propeller because of waves, current and vessel motions.

The SAFETUG [2], [3] project revealed that these reductions of line forces were significant for the azimuth stern drive (ASD) tug analysed in the project, whereas the Voith Water Tractor (VWT) had only small reductions due to its different seakeeping behaviour. There are two reasons for this: firstly, the Voith Schneider Propeller (VSP) is located deep inside the ship and secondly, VSPs are not affected by ventilation [4] because of the way in which thrust is generated.



Figure 2: Voith Schneider Propeller (X-ray view)

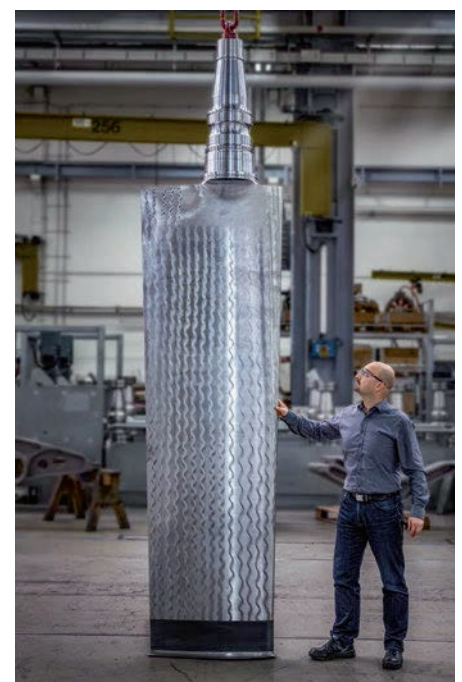


Figure 3: Blade size of a modern VSP (4-MW VSP unit)

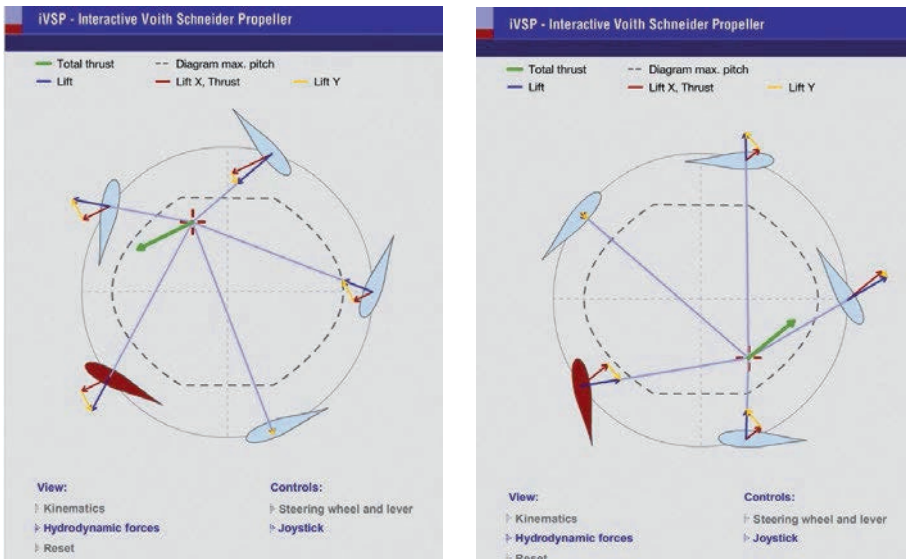


Figure 4: Thrust generation of a VSP: two thrust examples

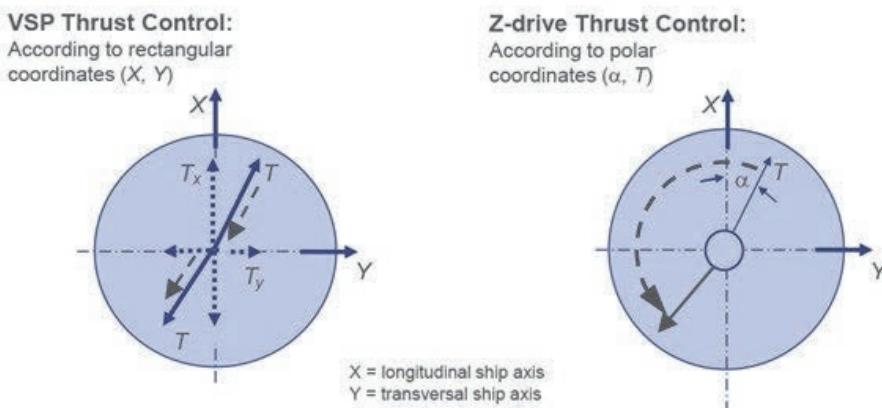


Figure 5: Thrust control principles of VSP and Z-drive thrusters

tended. Two tugs have been equipped with VRS so far: the offshore tug *Forte*, owned by Edison Chouest Offshore Inc (Figure 1), and the Japanese tug *Shinano Maru*.

### Functional principle of the VSP

The Voith Schneider Propeller is the ship's propulsion system. It provides fast and accurate thrust, steering and stabilisation forces simultaneously in both longitudinal and transverse directions. Figure 2 shows the inner structure of the VSP. Figure 3 shows the currently largest blade of a VSP for a 4-MW unit. The thrust is generated according to an X-Y logic. Unlike an azimuth thruster, longitudinal and transverse thrust can be generated independently of each other.

Figure 4 shows two thrust examples. Since only the amplitude and the phase

position of the blade oscillations have to be changed, thrust can be adjusted quickly.

In dynamic positioning (DP) mode, the X-Y logic has particular benefits because the force requirements of the DP system can be met quickly, separated into longitudinal and transverse thrust (Figure 5).

### Voith Roll Stabilization (VRS)

The VSP can generate thrust in longitudinal and transverse directions and can be adjusted quickly in terms of magnitude and direction, enabling the VSP to generate roll-stabilising moments, thereby reducing roll. When the vessel encounters an incoming wave, sensors measure the roll acceleration and the system immediately calculates and then applies the restoring force to counteract the rolling motion of the vessel. The working principle of VRS is explained in Figure 6 and Figure 7.

Bridge personnel can preselect the power range to be applied to roll stabilisation, which operates through the propeller both at zero speed – in DP mode, for example – or when the tug is under way.

Roll stabilising tanks are no longer required and thus there is no reduction of payload and the VRS can be integrated with other anti-roll systems if necessary. Increased uptime is supplemented by improved crew comfort and vessel safety.

### Simulation of roll damping

In order to quantify the effectiveness of the VRS, numerical roll damping simulations on a typical VWT have been conducted. Figure 8 shows the lines plan of the vessel. The main particulars are listed in Table 1. The tug is equipped with two VSPs with a blade orbit diameter of 3.2m, a blade length of 2.65m and a nominal input power of 2.7 MW each.

|                       |       |
|-----------------------|-------|
| $L_{wl}$ [m]          | 37.50 |
| $B_{wl}$ [m]          | 13.82 |
| $T$ [m]               | 3.75  |
| $D$ [m <sup>3</sup> ] | 1,242 |
| $GM$ [m]              | 3.41  |
| $r_{xx}/B$            | 0.297 |

Table 1: Main particulars

The project used simulation software, IMPRES, developed at the Institute of Fluid Dynamics and Ship Theory of the Technical University Hamburg and based on the Cummins equation [9]:

$$(\mathbf{M} + \mathbf{A}) \ddot{\xi} + \int_0^{\infty} \mathbf{B}(\tau) \dot{\xi}(t - \tau) d\tau + \mathbf{S} \xi(t) = \vec{F}(t)$$

This equation describes the motion of a ship over time due to arbitrary external forces  $\vec{F}(t)$ .  $\mathbf{M}$  and  $\mathbf{A}$  are matrices stating the ships inertia and added mass,  $\mathbf{S}$ , is a coefficient matrix for linear restoring forces and moments. The convolution integral models hydrodynamic damping forces and fluid memory effects due to radiated waves. Ogilvie [10] showed that this hydrodynamic radiation force can be determined using added mass and damping coefficients from efficient frequency domain calculations. For better numerical handling, IMPRES uses a modified version of the Cummins equation [11]:

$$(\mathbf{M} + \mathbf{A}) \ddot{\xi} + \vec{F}_B(\dot{\xi}, t) + \vec{F}_Q(\xi) + \mathbf{S}(\xi, t) = \vec{F}_{Wave}^{(1)}(t) + \vec{F}_{Ext}^{(1)}(t)$$



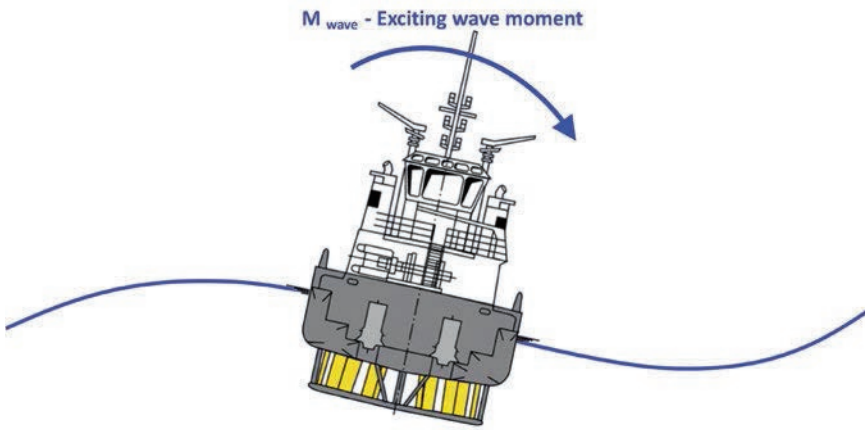


Figure 6: The exciting wave moment forces the tug to roll

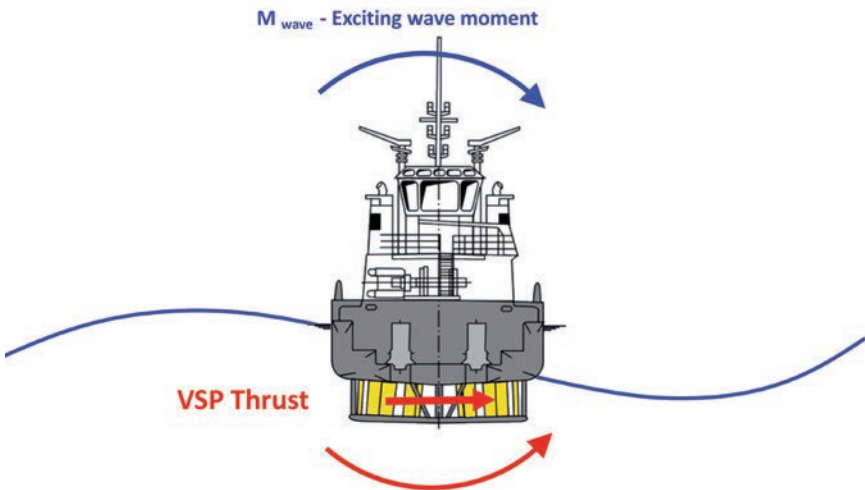


Figure 7: The fast reacting thrust of the VSP stabilises the tug

The convolution integral representing the retardation forces has been replaced with a more compact formulation ( $\vec{F}_B$ ), which also corresponds to the numerical structure of the code. A vector  $\vec{F}_Q$  to consider viscous damping contributions has been added. Instead of a linear restoring coefficient matrix, the restoring forces are described as a time- and motion-dependent vector

to capture their non-linear behaviour.  $\vec{F}_{Wave}^{(1)}$  states first-order wave excitation forces and  $\vec{F}_{Ext}$  represents time varying, arbitrary external loads.

**Hydrodynamic forces**

For an efficient determination of the hydrodynamic radiation and first-order wave excitation forces, frequency domain boundary

element methods based on potential theory are used in IMPRES.

In linear frequency domain methods, the forces acting on the ship's hull are separated into hydrodynamic mass and damping forces because of the movement of the hull in still water (radiation) and the hydrodynamic forces acting on a fixed ship hull in waves (excitation).

The wave excitation forces themselves can be interpreted as two components: Froude-Krilov forces, which originate from the instantaneous pressure distribution in the wave; and diffraction forces, which are caused by the disturbance of the wave flow due to the presence of the ship. All these sub-problems are treated separately and solved at discrete motion and wave frequencies to obtain hydrodynamic mass and damping coefficients and wave force response amplitude operators.

If only a small number of frequencies is used to evaluate the hydrodynamic damping over time, the retardation function matrices will show unphysical behaviour which results in unrealistic results and numerical instabilities. [11]. Therefore, the frequency-dependent hydrodynamic damping is approximated using a cubic spline interpolation to obtain more and equidistant sampling points and artificial boundary conditions are added. Since at zero frequency, there can be no velocity, the damping is set to zero. For high frequencies, the damping should also asymptotically tend to zero. The retardation function matrices are then integrated numerically and stored in the system's memory. At each time step, the damping forces arising from the retardation functions can then be simply evaluated as [11]:

$$\vec{F}_B(\dot{\xi}, t) = \int_0^\infty B(\tau) \dot{\xi}(t - \tau) d\tau$$

**Non-linear restoring forces**

$\vec{S}$  represents time-dependent restoring forces and moments. In every time step, the submerged volume and the centre of buoyancy is determined based on a sectional approach. Therefore the wetted hull surface is considered according to the actual sinkage, heel, and trim of the ship as well as the instantaneous wetted surface due to the incident waves [11]. Instead of using linearised restoring coefficients, this direct approach can capture non-linear effects like oscillating roll restoring moments between wave crest and trough which can cause parametric roll resonance.

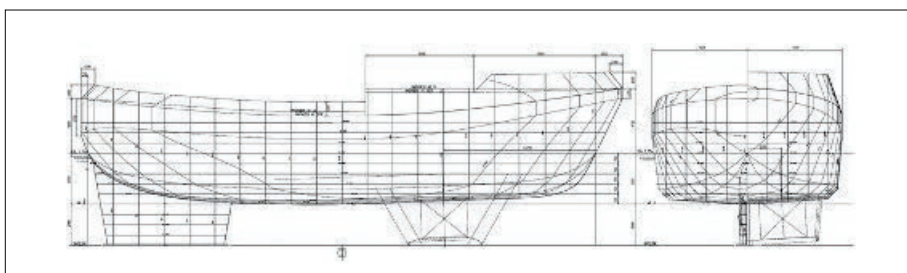


Figure 8: Lines plan of VWT

### Viscous damping contributions

In IMPRES, viscous roll damping contributions are considered using a quadratic damping moment  $M_\phi$  [12]:

$$M_\phi = (d_Q |\dot{\phi}| + d_L) \dot{\phi}$$

The linear and quadratic roll damping coefficients  $d_L$  and  $d_Q$  must be determined externally, e.g., by using model tests, viscous CFD calculations or other prediction methods. Particularly at low ship speeds, damping contributions due to flow separation at the hull edges cannot be neglected. In transverse direction, a section-based two-dimensional approach [13, 11] is used within the numerical simulation method. To consider low-speed damping effects in longitudinal direction, quadratic surge damping is added according to Fossen [14].

### Wave excitation in time domain

The first-order wave excitation in time domain  $\vec{F}_{Wave}^{(1)}(t)$  is calculated as the superposition of the excitation forces of the regular wave components [11,12].

### Validation

During the joint development of the simulation software by Technical University Hamburg and Voith, extensive seakeeping tests were undertaken on offshore vessels and tugs. Figure 9 shows the VWT model at a scale of 1:16.

Figure 10 shows a seakeeping test with an encounter angle of  $180^\circ$  (on the left). The tests were conducted in long-crested irregular waves according to a JONSWAP spectrum with a peak period  $T_p=8.57s$  and a significant wave height  $H_s=1.92m$ . The right-hand side of Figure 10 shows the corresponding snapshot of the seakeeping simulation. The same wave trains that had been generated by the wave maker in model tests were introduced in the simulation.

Figure 12 shows the wave height over time (100s section) for both model tests and simulation. The simulated waves are almost identical to the measured ones. The main degree of freedom that is excited in this configuration is pitch motion. The main features of the measured signal are reproduced well by the numerical method which slightly overpredicts the peaks of the pitch motion but is considered good enough to study the different variants in active roll damping.

### Roll decay

The numerical approach does not consider any viscous effects. However, these >

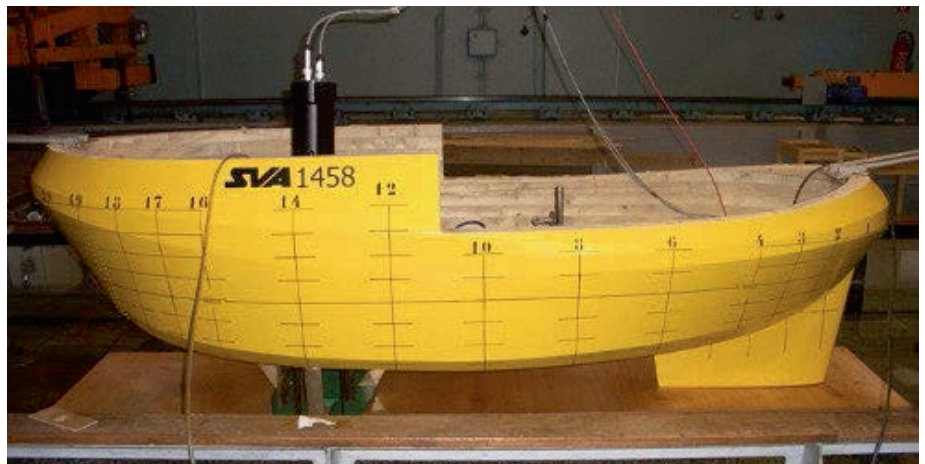


Figure 9: VWT in model scale

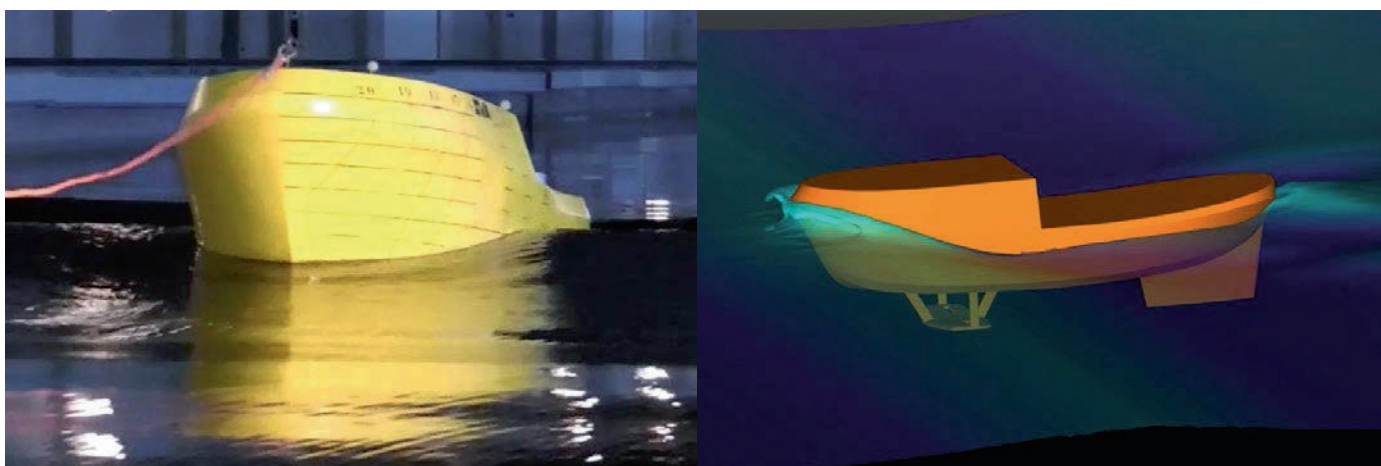


Figure 10: Seakeeping test and simulation

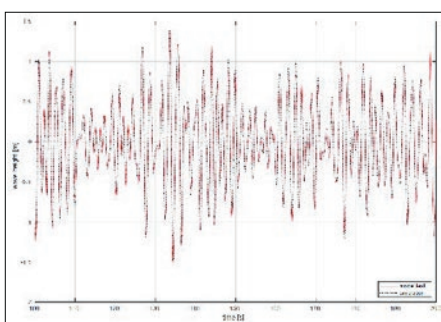


Figure 11: Wave height over time (red solid: model test, black dotted: simulation)

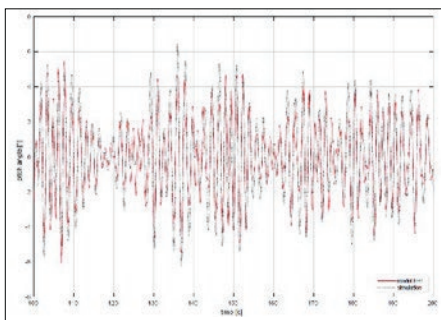


Figure 12: Pitch angle over time (red solid: model test, black dotted: simulation)

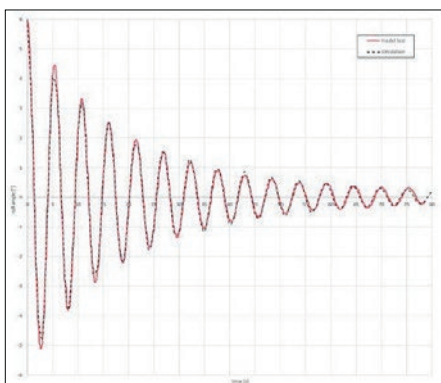


Figure 13: Roll decay: comparison of model test and simulation

can make a significant contribution to roll damping and can be accounted for by introducing viscous roll damping coefficients derived from a roll decay test, for example. There the vessel is deflected to a static heel angle and released so it executes a damped decaying roll motion in its natural frequency.

The red curve in Figure 13 shows the time series of such a test. The logarithmic reduction of subsequent roll amplitudes is a measure for the damping capacity of the vessel.

The linear and quadratic damping coefficients have been derived as

$$d_L = 1331 \text{ kNm/s}$$

$$d_Q = 18,000 \text{ kNm/s}^2$$

The black dotted curve in Figure 13 represents the simulation of the roll decay test with a satisfactory agreement.

#### Roll damping simulations

For the simulation of active roll damping, IMPRES is embedded into a more complex environment comprising of a proportional derivative controller to provide the thrust figures dependent on the roll rate. These thrust figures are processed by an allocation module that converts the required thrust into VSP settings for pitch. The delivered propeller forces are then fed into the motion solver as additional forces acting on the vessel next to the wave forces.

All simulations were carried out with three wave realisations of three hours duration each. The significant wave height was  $H_s = 2.5\text{m}$  with a peak period of  $T_p = 6.87\text{s}$ . The encounter angle was set to  $90^\circ$  (beam seas). The power available to the propellers was limited to 30% of the nominal power.

Figure 14 presents the time series of the tug's roll angle over 500s real time with Voith Roll Stabilization off (blue) and on (red) over one wave realisation. It is clear that the damping moment of the propellers contributes quite significantly to the reduction of the roll angle.

Corresponding simulations have been carried out for different peak periods of the wave spectrum as well as several limitations of power available to the VRS. Figure 15 summarises the results. The blue dotted line shows the vessel response of the significant roll angle without any damping actions. The resonance peak at  $T_p = 7\text{s}$  is clearly visible. The excitation frequency equals the natural frequency of the vessel for roll motion. The remaining curves represent the significant roll angle with Voith Roll Stabilization activated at different power limits. At resonance frequency the roll response of the vessel reduces from  $22^\circ$  to below  $7^\circ$  already for a power limit of 30% maximum continuous rating (MCR).

Figure 16 shows the relative roll reduction of the same scenario. It is clear that the VRS can achieve roll reduction figures greater than 70% over a large range of wave periods. It therefore offers significant scope to widen operational weather windows.

The mean power consumption during the three hour simulation run is shown in Figure 17 over the different wave periods.

#### Summary

The SAFETUG study demonstrated that rolling is often a limiting factor in tug operation, particularly at offshore terminals. This analysis has shown that with its fast and precise thrust control, the Voith Schneider Propeller enables a significant reduction in rolling motion.



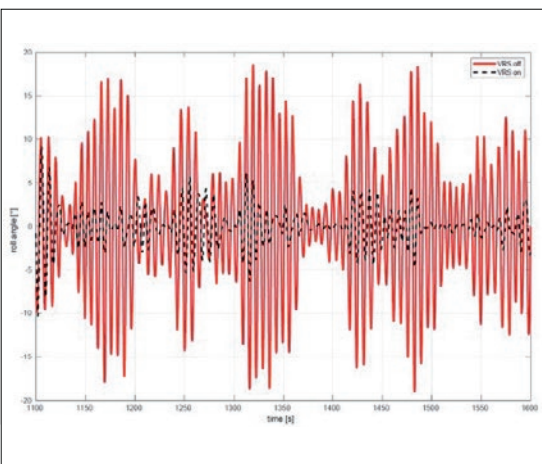


Figure 14: Time series of roll angle (blue: VRS off, red: VRS on)

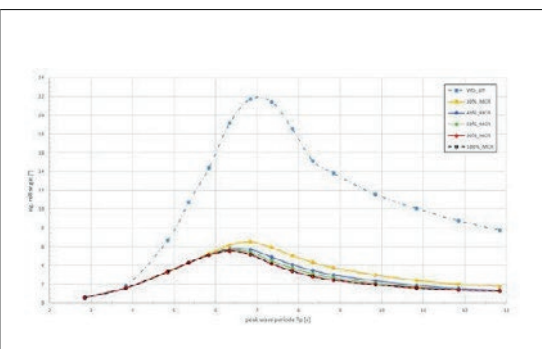


Figure 15: Roll angle without (dotted) and with VRS at different power levels (solid)

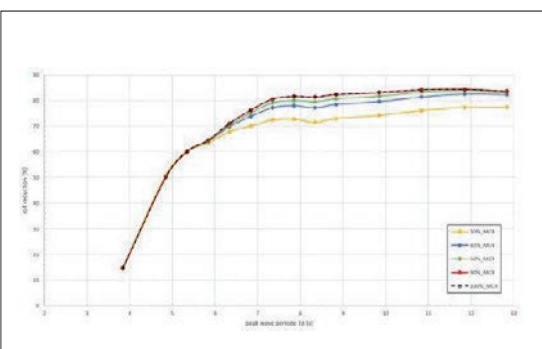


Figure 16: Roll reduction by VRS at 30% MCR

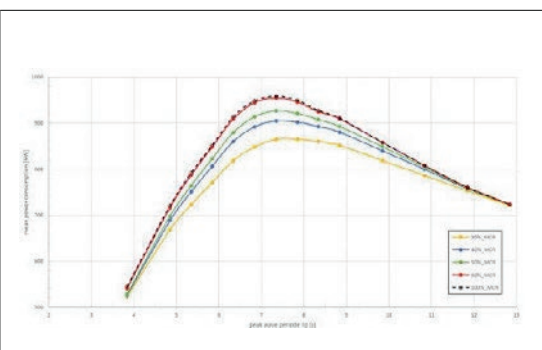


Figure 17: Mean power consumption at different power limits

In model tests and calculations in the time domain, it was shown that rolling motion can be significantly reduced, by as much as 80%, when tugs are both stationary and in transit. The calculation results correlate closely with the practical experience on board the offshore tug, *Forte*, belonging to Edison Chouest Offshore.

### References

[1] H. Hensen, Tug use in port, A practical guide including ports, ort approaches and offshore terminals, Trowbridge: ABR company Ltd., 2018.  
 [2] "https://www.marin.nl/jips/safetug-i," [Online].  
 [3] "https://www.marin.nl/jips/safetug-ii," [Online].  
 [4] M. Palm, D. Jürgens and D. Bendl, "Numerical and Experimental Study on Ventilation for Azimuth Thrusters and

Cycloidal Propellers," in Second International Symposium on Marine Propulsors, smp'11, Hamburg, 2011.  
 [5] B. Buchner, P. Dierx and O. Waals, "The behavior of tugs in waves assisting LNG carriers during berthing along offshore LNG terminals," in Proceedings of OMAE 2005, Halkidiki, 2005.  
 [6] J. Ögge, "Global shipping trends and the Carrousel RAVE Tug: Connecting the dots," in ITS, Marseille, 2018.  
 [7] D. Jürgens and M. Palm, "Influence of Thruster Response Time on DP Capability by Time-Domain Simulations," in Dynamic Positioning Conference, Houston, 2017.  
 [8] "https://voith.com/bridge/index.html," [Online].  
 [9] W. Cummins, "The Impulse Response Function and Ship Motions," 1962.  
 [10] T. Oglvie, "Recent Progress towards the Understanding and Prediction of Ship Motions," in Proceedings of the 5th Symposium on Naval Hydrodynamics, 1964.  
 [11] O. Detlefsen, Entwicklung eines Verfahrens zur Simulation von Schiffsbewegungen und dynamischem Positionieren im Seegang unter Verwendung von Impuls-Antwort-Funktionen, 2014.  
 [12] H. Kröger, "Simulation der Rollbewegung von Schiffen im Seegang," 1987.  
 [13] J. Brix, Manoeuvring Technical Manual, 1992.  
 [14] T. Fossen, Handbook of Marine Craft Hydrodynamics and Motion Control, 2011.

Voith Group  
St. Poeltener Str. 43  
89522 Heidenheim, Germany

Contact:  
Phone +49 7321 37-2055  
[vspmarine@voith.com](mailto:vspmarine@voith.com)  
[www.voith.com](http://www.voith.com)



**VOITH**